Monte Carlo computation of the Laplace transform of exponential Brownian functionals

Nicolas Privault[*]   Wayne Isaac Uy[†]

School of Physical and Mathematical Sciences
Nanyang Technological University
SPMS-MAS, 21 Nanyang Link
Singapore 637371

October 13, 2011

Abstract

This paper is concerned with the Monte Carlo numerical computation of the Laplace transform of exponential Brownian functionals. In addition to the implementation of standard integral formulas, we investigate the use of various probabilistic representations. This involves in particular the simulation of the hyperbolic secant distribution and the use of several variance reduction schemes. The performance of those methods and their conditions of application are compared.

Key words: Exponential Brownian functionals, Monte Carlo method, generalized hyperbolic secant distribution.
Mathematics Subject Classification (2010): 65C05, 33C10, 60J60, 65C10, 35Q40.

1   Introduction

Exponential Brownian functionals of the form

$$\mathcal{A}_\tau = \int_0^\tau e^{\sigma B_s + \rho \sigma^2 s/2} ds, \qquad \rho \in \mathbb{R}, \quad \tau \geq 0, \tag{1.1}$$

---

[*]nprivault@ntu.edu.sg
[†]wa0001uy@e.ntu.edu.sg

where $(B_s)_{s\in\mathbf{R}_+}$ is a standard Brownian motion, play an important role in the statistical physics of disordered systems where $\mathcal{A}_\tau$ is the partition function and $\log\mathcal{A}_\tau$ represents the free energy of the system. They are also used in financial mathematics for the pricing of Asian options and of bonds in interest rate models, cf. e.g. [2], [13], and references therein.

The Laplace transform

$$F_\rho(\tau,x) = E\left[\exp\left(-x\int_0^\tau e^{\sigma B_s + \rho\sigma^2 s/2}ds\right)\right], \qquad \rho\in\mathbf{R}, \quad x\in\mathbf{R}_+, \qquad (1.2)$$

of $\mathcal{A}_\tau$, $\tau\geq 0$, can be shown to satisfy the PDE

$$\begin{cases} \dfrac{\partial F_\rho}{\partial\tau}(\tau,x) = \dfrac{1}{2}\sigma^2 x^2\dfrac{\partial^2 F_\rho}{\partial x^2}(\tau,x) + \lambda x\dfrac{\partial F_\rho}{\partial x}(\tau,x) - xF_\rho(\tau,x) \\[2mm] F_\rho(0,x) = 1, \qquad x\in\mathbf{R}_+, \end{cases} \qquad (1.3)$$

whose solution has been computed in [14] using spectral expansions as

$$F_\rho(\tau,x)$$
$$= \frac{\sigma^\rho}{2\pi^2(2x)^{\rho/2}}\int_0^\infty \sin\left(\frac{\sqrt{8x}}{\sigma}\sinh a\right)\int_0^\infty ue^{-\sigma^2(\rho^2+u^2)\tau/8}\cosh\left(\frac{\pi u}{2}\right)\left|\Gamma\left(\frac{\rho}{2}+i\frac{u}{2}\right)\right|^2\sin(ua)du\,da$$
$$-\frac{\sigma^\rho}{(2x)^{\rho/2}}\sum_{0\leq k<-\rho/2}\frac{2(\rho+2k)}{k!\Gamma(1-\rho-k)}e^{\sigma^2 k(k+\rho)\tau/2}K_{-\rho-2m}\left(\frac{\sqrt{8x}}{\sigma}\right), \qquad (1.4)$$

where

$$K_w(t) = \int_0^\infty e^{-t\cosh x}\cosh(wx)dx, \qquad t\in\mathbf{R},$$

is the modifed Bessel function of the second kind with parameter $w\in\mathbb{C}$. This expression is commonly used in the mathematical physics literature, cf. e.g. [3], as well as in mathematical finance [10].

On the other hand, the probability density of $\mathcal{A}_t$ has been computed for $z>0$ as

$$\Psi_\rho(\tau,z) = \frac{\sigma}{2z}e^{-\rho^2\sigma^2\tau/8-2\sigma^{-2}/z}\int_{-\infty}^\infty \exp\left(\frac{\rho\sigma}{2}y - \frac{2}{\sigma^2}\frac{e^{\sigma y}}{z}\right)\theta\left(\frac{4e^{\sigma y/2}}{\sigma^2 z},\frac{\sigma^2\tau}{4}\right)dy, \quad (1.5)$$

in [16], Proposition 2, cf. also [11], where $\theta(v,\tau)$ is the positive function

$$\theta(v,\tau) = \frac{ve^{\pi^2/(2\tau)}}{\sqrt{2\pi^3\tau}}\int_0^\infty e^{-\xi^2/(2\tau)}e^{-v\cosh\xi}\sinh(\xi)\sin\left(\pi\xi/\tau\right)d\xi, \qquad v,\tau>0, \quad (1.6)$$

which leads to various integral representations of $F_\rho(\tau, x)$, cf. (2.1), (2.2), (2.3) below. Numerical computations of the density (1.5) of $\mathcal{A}_t$ have been presented in [7], based on the evaluation of the function $\theta(v, \tau)$ by the Fast Fourier Transform (FFT). It has been noted in particular in [7] that the numerical evaluation of $\theta(\tau, x)$ is difficult for small values of x, see for example Figure 2 therein for $\tau = 0.5$ in which the FFT can yield negative values for the positive function $x \mapsto \theta(0.5, x)$.

The solution $F_\rho(\tau, x)$ can also be computed by the Monte Carlo method and simulation of Brownian paths in (1.2). Another expression suitable for Monte Carlo simulation is

$$F_\rho(\tau, x) = \Gamma(\rho) \left(\frac{\sigma}{\sqrt{8x}} \right)^\rho e^{-\sigma^2 \tau \rho^2 / 8} E \left[Z_\rho^2 e^{-\sigma^2 \tau Z_\rho^2 / 8} \text{sinhc}(Z_\rho) K_{i Z_\rho}(\sqrt{8x}/\sigma) \right], \quad (1.7)$$

$x > 0$, $\tau > 0$, where Z_ρ is a random variable having the generalized hyperbolic secant (GHS) distribution with parameter $\rho > 0$, and sinhc is the hyperbolic sine cardinal function, cf. Corollary 3.3 of [13].

In this paper we focus on the implementation of (1.7) by the Monte Carlo method, in addition to the numerical computation of $F_\rho(\tau, x)$ using integral representations based on (1.4) and (1.5), cf. [9] for a preliminary approach. The performance of Monte Carlo estimators is compared by their respective root mean square errors. The performance of the integral method versus that of Monte Carlo algorithms is more difficult to compare since the two methods are different in nature and have distinct advantages.

In Section 2 we consider the computation of the Laplace transform from the point of view of integral representations. In particular we compare the performance of the integral representations (2.1), (2.2), (2.3), obtained from the probability density of $\mathcal{A}_\tau$ and from heat kernels, cf. (1.4), (2.6). In Section 3 we consider several computations of the Laplace transform by the Monte Carlo method via Relations (1.2) and (1.7). In particular we investigate the numerical implementation of the Monte Carlo method using the generalized hyperbolic secant distribution, to which variance reduction schemes are applied.

2   Integral method

Density approach

The Laplace transfom $F_\rho(\tau, x)$ can be computed for all $\rho \in \mathbb{R}$ by applying (1.5) to the computation of the expectation (1.2), as follows:

$$F_\rho(\tau, x) = e^{-\sigma^2\rho^2\tau/8} \int_0^\infty \int_0^\infty e^{-ux} \exp\left(-\frac{2\left(1+z^2\right)}{\sigma^2 u}\right) \theta\left(\frac{4z}{\sigma^2 u}, \frac{\sigma^2\tau}{4}\right) \frac{du}{u} \frac{dz}{z^{1-\rho}}. \quad (2.1)$$

The above formula involves a triple integral which can be difficult to evaluate in practice. The next formula provides an alternative expression for the solution $F_\rho(\tau, x)$ using a double integral, which is however valid only for $\rho > -1$, cf. Corollary 2.3 of [13]:

$$F_\rho(\tau, x) = 2e^{-\sigma^2\rho^2\tau/8} \int_0^\infty \left(v^2 + 8x/\sigma^2\right)^{-\rho/2} \theta\left(v, \frac{\sigma^2\tau}{4}\right) K_{-\rho}\left(\sqrt{v^2 + 8x/\sigma^2}\right) \frac{dv}{v^{1-\rho}}. \quad (2.2)$$

In Figure 2.1 below we present an implementation of (2.2) using the composite Simpson rule. The values obtained for $\tau < 5$ were out of the $[0, 1]$ range, and are not shown in the graph.
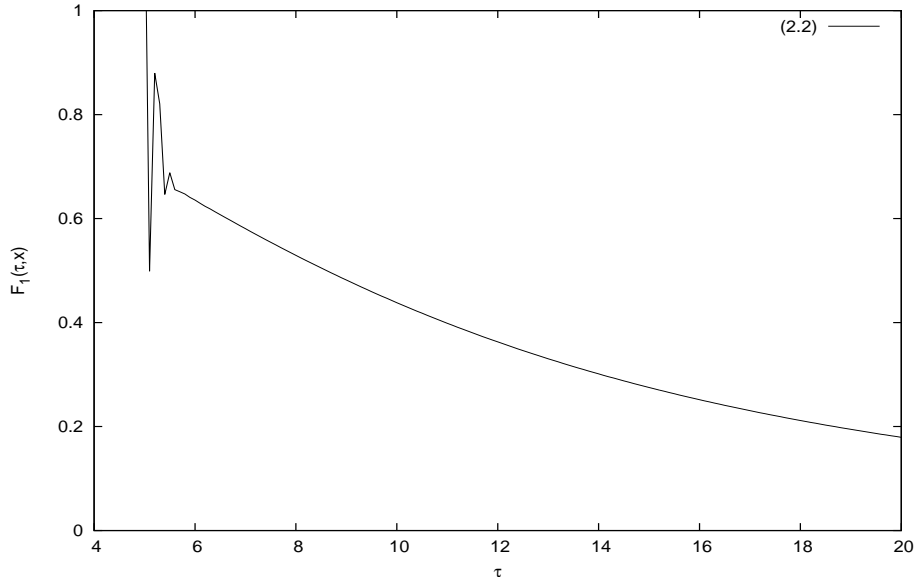

Figure 2.1: $F_1(\tau, x)$ computed with $x = 0.06$ and $\sigma = 0.3$.

The numerical evaluation of (2.2) involves the function $\theta(\tau, x)$ which is difficult to evaluate in practice, especially for small values of x and t, cf. [7]. The use of the FFT

for the computation of $\theta(\tau, x)$ did not significantly improve the precision and in this respect we only confirmed the results of [7], cf. Figure 2 therein.

The next formula

$$
\begin{aligned}
F_\rho(\tau, x) &= \frac{8}{\sigma^2 \pi^{3/2}} \sqrt{\frac{x}{\tau}} e^{-\sigma^2 \rho^2 \tau/8 + 2\pi^2/(\sigma^2 \tau)} \\
&\int_0^\infty z^\rho \int_0^\infty e^{-2\xi^2/(\sigma^2\tau)} \frac{\sinh(\xi) \sin\left(4\pi\xi/(\sigma^2\tau)\right)}{\sqrt{(z+\xi)(z+\xi^{-1})}} K_1\left(\sqrt{8x}\sqrt{(z+\xi)(z+\xi^{-1})}/\sigma\right) d\xi dz
\end{aligned}
\tag{2.3}
$$

is an alternative representation formula that involves only double integrals and special functions for all $\rho \in \mathbb{R}$, cf. Corollary 2.2 of [13]. We attempted to compute (2.3) by numerical quadrature and using the composite midpoint rule for the outer dz-integral as the integrand is not defined at the end points. However, most of the computed values of $F_\rho(\tau, x)$ are outside of the $[0, 1]$ range, suggesting that more sophisticated quadrature rules have to be implemented.

The density $\Psi_\rho(\tau, z)$ can also be computed by inversion of its Laplace transform, using Whittaker functions and generalized Laguerre polynomial, cf. Proposition 2.3 of [12]. Another integral representation has been obtained in [6] using hypergeometric functions, however both expressions are difficult to compute numerically due to the presence of hypergeometric functions.

Heat kernel approach

The Laplace transform $F_\rho(\tau, x)$ can be written for all $\rho \in \mathbb{R}$ as

$$
F_\rho(\tau, x) = \frac{2^{1-\rho}\sigma^\rho}{\pi(\sqrt{2x})^\rho} e^{-\rho^2\sigma^2\tau/8} \int_0^\infty e^{\rho y} \int_0^\infty u^2 \mathrm{sinhc}(u) e^{-u^2\sigma^2\tau/8} K_{iu}(\sqrt{8x}/\sigma) K_{iu}(e^y) du dy,
\tag{2.4}
$$

$x > 0$, $\tau > 0$, cf. Proposition 3.1 of [13], where sinhc is the hyperbolic sine cardinal function

$$
\mathrm{sinhc}x = \frac{\sinh(\pi x)}{\pi x}, \qquad x \in \mathbb{R},
$$

and

$$
K_{iu}(x) = \frac{1}{\sinh(\pi u/2)} \int_0^{+\infty} \sin(x \sinh a) \sin(ua) da, \qquad x \in \mathbb{R}_+, \quad u \in \mathbb{R}, \tag{2.5}
$$

cf. e.g. [15] pp. 182-183.

From a computational point of view the above formula actually involves a triple integral of a Bessel function, which can be simplified to a double integral of a Gamma function, as

$$
\begin{aligned}
F_\rho(\tau, x) = & \frac{\sigma^\rho}{2\pi(2x)^{\rho/2}} \int_0^\infty u^2 e^{-\sigma^2(\rho^2+u^2)\tau/8} \text{sinhc}(u) \left| \Gamma\left(\frac{\rho}{2} + i\frac{u}{2}\right) \right|^2 K_{iu}\left(\frac{\sqrt{8x}}{\sigma}\right) du \\
& - \frac{\sigma^\rho}{(2x)^{\rho/2}} \sum_{k=0}^\infty \frac{2(2k+\rho)^-}{k!\Gamma(1-\rho-k)} e^{\sigma^2 k(k+\rho)\tau/2} K_{-\rho-2k}\left(\frac{\sqrt{8x}}{\sigma}\right),
\end{aligned}
\tag{2.6}
$$

for all $\rho \in \mathbb{R}$, $x > 0$, and $\tau > 0$, which recovers (1.4) under (2.5).

We computed the above integrals by the composite Simpson rule. The complex Gamma function was computed in the <complex> class from [17]*, and the modified Bessel function K_v of the second kind, $v \in \mathbb{R}$, was computed using the Irregular Modified Bessel Functions of Fractional Order gsl_sf_bessel_Knu function of the GNU Scientific Library (GSL).[†]

We used 20 as the upper bound in the du-integral in (2.6). Concerning the integral (2.5) for K_{iu} we note that $F_\rho(\tau, x)$ is more sensitive to changes in the upper bound A when approximating (2.5) by

$$
K_{iu}(x) \simeq \frac{1}{\sinh(\pi u/2)} \int_0^A \sin(x \sinh a) \sin(ua) da, \qquad x \in \mathbb{R}_+, \quad u \in \mathbb{R}.
$$

This is due to the fact that the integrand in (2.5) is oscillating while $u^2 e^{-u^2}$ in (2.6) decreases at a fast rate to 0.

---

[*]https://www.crbond.com/math.htm
[†]https://www.gnu.org/software/gsl/manual/html_node/Irregular-Modified-Bessel-Functions-_002d-Fractional-Order.html
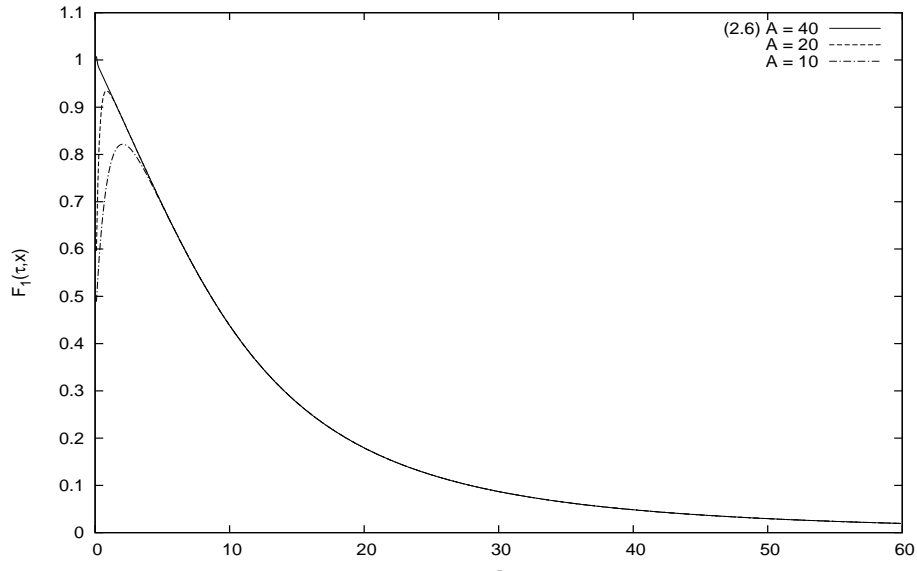
Figure 2.2: $F_1(\tau, x)$ computed with $x = 0.06$ and $\sigma = 0.3$.

Figure 2.2 above shows the graph of the values obtained from (2.6) for different values of the upper bound A in (2.5), and shows that using $A = 40$ yields satisfying values for $F_\rho(\tau, x)$. In addition it solves the divergence problem encountered in the implementation of (2.2) for small values of τ in Figure 2.1.

In applications to bond pricing, $F_\rho(\tau, x)$ can be interpreted as the price

$$F_\rho(\tau, r_0) = E\left[\exp\left(-\int_0^\tau r_s ds\right)\right], \qquad \tau \geq 0, \tag{2.7}$$

of a bond in the Dothan geometric short rate model $r_s = r_0 e^{\sigma B_s + \rho \sigma^2 s / 2}$, $s \in \mathbb{R}_+$, cf. [13]. Here, τ represents the maturity time of a bond, r_s is the underlying interest rate value at time $s \in \mathbb{R}_+$, and $F_\rho(\tau, r_0)$ is the bond price under the condition $F_\rho(0, r_0) = \$1$, which means that the bond can be redeemed at its face value at the date of maturity τ.

For example, assuming a volatility coefficient of $\sigma = 30\%$, and a drift value of $\rho \sigma^2 / 2 = 0.045$ per year in (1.1), the price of a zero-coupon bond ten years before maturity equals \$0.43 in this model when the underlying short term interest rate is at 6%.

3   Monte Carlo method

The Laplace transform $F_\rho(\tau, x)$ can be computed by Monte Carlo estimation of the expression

$$F_\rho(\tau, x) = E\left[\exp\left(-x\int_0^\tau e^{\sigma B_s + \rho\sigma^2 s/2}ds\right)\right], \qquad \tau \geq 0, \qquad (3.1)$$

after discretization of the stochastic integral over $[0, \tau]$. As noted in the introduction, it can also be computed for $\rho > 0$ by the relation

$$F_\rho(\tau, x) = \Gamma(\rho)\left(\frac{\sigma}{\sqrt{8x}}\right)^\rho e^{-\sigma^2\tau\rho^2/8}E\left[Z_\rho^2 e^{-\sigma^2\tau Z_\rho^2/8}\text{sinhc}(Z_\rho)K_{iZ_\rho}(\sqrt{8x}/\sigma)\right], \quad (3.2)$$

$x > 0$, $\tau > 0$, cf. (1.7) above. The proof of (3.2) follows directly from (2.6) and the expression

$$f_\rho(x) = \frac{2^{\rho-2}}{\pi\Gamma(\rho)}\left|\Gamma\left(\frac{\rho}{2} + i\frac{x}{2}\right)\right|^2, \qquad x \in \mathbb{R}, \qquad (3.3)$$

of the generalized hyperbolic secant (GHS) density of Z_ρ with characteristic function $u \mapsto (\cosh u)^{-\rho}$, $\rho > 0$, see also the proof of Proposition 3.1 below.

Among other advantages, the Monte Carlo method allows for the reuse of stored samples for different values of the parameters, and for the randomization of parameters inside the integral. In applications to finance the initial condition r_0 in in the Dothan geometric short rate model $r_s = r_0 e^{\sigma B_s + \rho\sigma^2 s/2}$ can be made random, e.g. when pricing default bonds via (2.7). In this case the implementation of the Monte Carlo can be preferred to the integral discretization due to the possibility of reusing the same samples of Z_ρ when simulating different values of r_0. In addition, in comparison with (1.2) and (3.1), Formula (3.2) also allows for the reuse of stored random samples of Z_ρ for different values of both $x > 0$ and $\tau > 0$ as the law of Z_ρ depends only on ρ, cf. e.g. Figure 3.4 below.

Next we discuss the generation of random samples of Z_ρ for the Monte Carlo computation of (3.1) and (3.2).

Simulation of the generalized hyperbolic secant distribution

(*i*) Inverse function method

When $\rho = 1$ the expression (3.3) simplifies to the hyperbolic secant density

$$f_1(x) = \frac{1}{2}\text{sech}\left(\frac{\pi}{2}x\right) = \frac{1}{2\cosh\left(\pi x/2\right)}, \qquad x \in \mathbf{R}, \qquad (3.4)$$

with distribution function

$$x \longmapsto \frac{2}{\pi}\arctan\left(\exp(\pi x/2)\right), \qquad x \in \mathbf{R}. \qquad (3.5)$$

In this case, samples of Z_1 can be generated from a uniform random variable U as

$$Z_1 = \frac{2}{\pi}\log\tan(\pi U/2)$$

by the inverse function method based on (3.4) and (3.5). The $U(0,1)$ generator[‡] of [8] has been used in the simulations.

(*ii*) Rejection method

When $\rho \neq 1$ the inversion method can no longer be applied, and we have used the rejection algorithm of [4] for log-concave probability densities when $\rho \gg 0.5$, as the GHS density appears to be log-concave in this parameter range. We also tested the rejection algorithms of [5] based on (3.3). In that case the rejection with perfect asymptotic fit, which is valid for $\rho \geq 1$, has been preferred to the direct rejection method of [5] which is valid for all $\rho > 0$, and whose performance was found to be lower.

In Figure 3.1 we compare the results of (3.1) and (3.2) for $\rho = 4$. In Figure 3.1, 2500 samples were used for (3.1) with a root mean square error of 4.24E-5, while 25000 samples were used for (3.2) with a root mean square error of 5.55E-7 and a similar computation time. This shows that for large values of τ in (3.1), the expression (3.2) yields a better result than (3.1), i.e. a root mean square error reduced by a factor 76.

[‡]`https://cg.scs.carleton.ca/~luc/rng.html`

The algorithm of Figure 2.2 was used as a reference when computing the above root mean square errors for the Monte Carlo method.
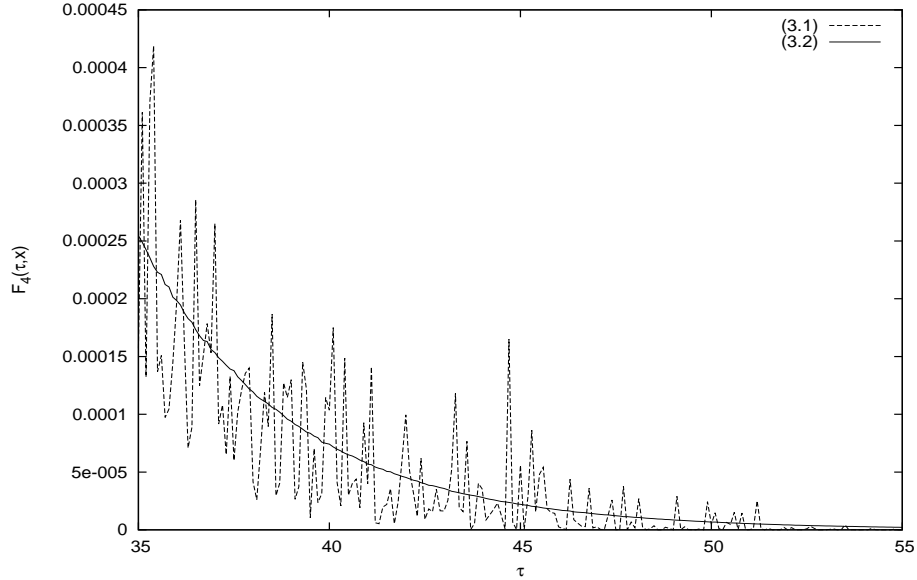

Figure 3.1: Computation of $F_4(\tau, x)$ by (3.1) and (3.2) with $x = 0.06$ and $\sigma = 0.3$.

In Figure 3.2 the expression (3.1) is simulated using 10000 samples with a root mean square error of 1.70E-3, while (3.2) is simulated with 65000 samples and yields a root mean square error of 0.47 for a similar computation time.
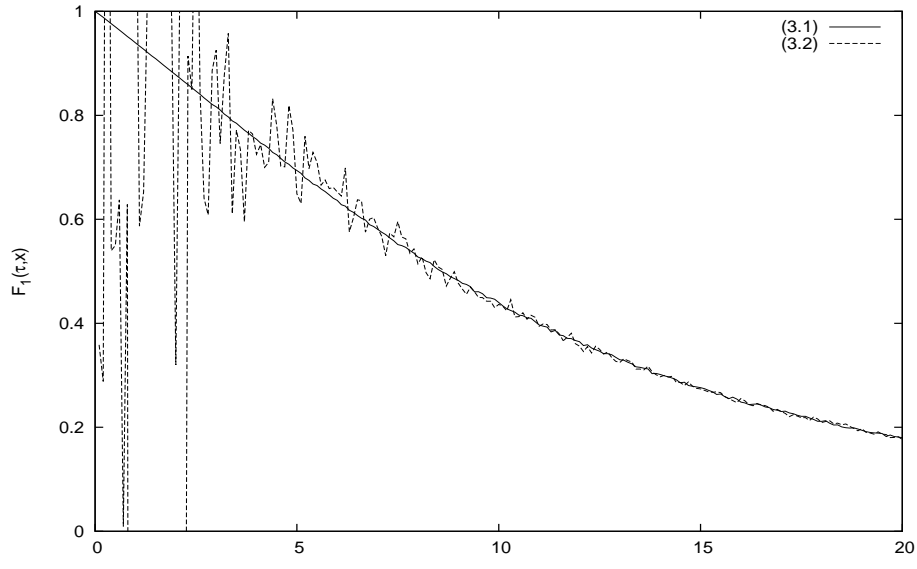

Figure 3.2: Computation of $F_1(\tau, x)$ by (3.1) and (3.2) with $x = 0.06$ and $\sigma = 0.3$.

This shows that for small values of τ, (3.1) yields a better precision than (3.2) by

improving the root mean square error by a factor 275. Indeed, the variance of the estimator in (3.2) is greater for small values of $\tau > 0$, and this tends to degrade the performance of the Monte Carlo estimator. This problem will be tackled by employing various variance reduction schemes.

When calculating $K_{iu}(x)$ in Monte Carlo simulations, we opted for the series representation

$$K_z(x) = \frac{\pi}{2\sin(\pi z)}(I_{-z}(x) - I_z(x)), \qquad x \in \mathbb{R}, \quad z \in \mathbb{C},$$

where

$$I_z(x) = \sum_{l=0}^{\infty} \frac{1}{l!(l+z)!}\left(\frac{x}{2}\right)^{z+2l}, \qquad x \in \mathbb{R}, \quad z \in \mathbb{C}, \tag{3.6}$$

The factorial in the series representation (3.6) was computed using the C codes for the complex Gamma function based on [17].§

Next we implement various algorithms in order to solve the problem of increasing variance for small values of τ in (3.2).

Variance reduction

(i) Importance sampling

We start by applying importance sampling, based on the fact that for $\rho^* > \rho > 0$ the likelihood ratio

$$
\begin{aligned}
x \mapsto \frac{f_\rho(x)}{f_{\rho^*}(x)} &= 2^{\rho-\rho^*}\frac{\Gamma(\rho^*)}{\Gamma(\rho)}\frac{\left|\Gamma\left(\frac{\rho}{2}+i\frac{x}{2}\right)\right|^2}{\left|\Gamma\left(\frac{\rho^*}{2}+i\frac{x}{2}\right)\right|^2} \\
&= \frac{2^{\rho-\rho^*}\Gamma(\rho^*)}{\Gamma(\rho)|\Gamma((\rho^*-\rho)/2)|^2}\left|B\left(\frac{\rho}{2}+i\frac{x}{2},\frac{\rho^*}{2}-\frac{\rho}{2}\right)\right|^2
\end{aligned}
$$

decreases to 0 as $|x|$ becomes large, where $B(x,y) = \Gamma(x)\Gamma(y)/\Gamma(x+y)$ denotes the Beta function, therefore reducing the importance of large sample values of Z_{ρ^*}.

In the next Proposition 3.1, Z_{ρ^*} denotes a GHS random variable with parameter $\rho^* > \rho > 0$.

---

§https://www.crbond.com/math.htm

Proposition 3.1 *For all $\rho^* > \rho > 0$ we have*

$$F_\rho(\tau, x) = \frac{2^{-\rho^*}\Gamma(\rho^*)}{\Gamma((\rho^* - \rho)/2)^2} \left(\frac{\sigma}{\sqrt{2x}}\right)^\rho \tag{3.7}$$

$$\times E\left[Z_{\rho^*}^2 e^{-\sigma^2(\rho^2 + Z_{\rho^*}^2)\tau/8} \left|B\left(\frac{\rho}{2} + i\frac{Z_{\rho^*}}{2}, \frac{\rho^* - \rho}{2}\right)\right|^2 \mathrm{sinhc}(Z_{\rho^*}) K_{iZ_{\rho^*}}(\sqrt{8x}/\sigma)\right],$$

$x > 0$, $\tau > 0$.

Proof. For all $\rho^* > \rho > 0$ we have

$$F_\rho(\tau, x)$$

$$= \Gamma(\rho)\left(\frac{\sigma}{\sqrt{8x}}\right)^\rho e^{-\sigma^2\tau\rho^2/8} E\left[Z_\rho^2 e^{-\sigma^2\tau Z_\rho^2/8}\mathrm{sinhc}(Z_\rho)K_{iZ_\rho}(\sqrt{8x}/\sigma)\right]$$

$$= \frac{1}{2\pi}\left(\frac{\sigma}{\sqrt{8x}}\right)^\rho \int_0^\infty u^2 e^{-\sigma^2(\rho^2+u^2)\tau/8}\mathrm{sinhc}(u)\left|\Gamma\left(\frac{\rho}{2} + i\frac{u}{2}\right)\right|^2 K_{iu}\left(\frac{\sqrt{8x}}{\sigma}\right)du$$

$$= \frac{1}{2\pi}\left(\frac{\sigma}{\sqrt{8x}}\right)^\rho \int_0^\infty u^2 e^{-\sigma^2(\rho^2+u^2)\tau/8}\mathrm{sinhc}(u)\left|\Gamma\left(\frac{\rho^*}{2} + i\frac{u}{2}\right)\right|^2 \frac{\left|\Gamma\left(\frac{\rho}{2} + i\frac{u}{2}\right)\right|^2}{\left|\Gamma\left(\frac{\rho^*}{2} + i\frac{u}{2}\right)\right|^2} K_{iu}\left(\frac{\sqrt{8x}}{\sigma}\right)du$$

$$= \frac{\Gamma(\rho^*)}{2^{\rho^*}}\left(\frac{\sigma}{\sqrt{8x}}\right)^\rho e^{-\sigma^2\rho^2\tau/8} E\left[Z_{\rho^*}^2 e^{-\sigma^2\tau Z_{\rho^*}^2/8}\frac{\left|\Gamma\left(\frac{\rho}{2} + i\frac{Z_{\rho^*}}{2}\right)\right|^2}{\left|\Gamma\left(\frac{\rho^*}{2} + i\frac{Z_\rho^*}{2}\right)\right|^2}\mathrm{sinhc}(Z_{\rho^*})K_{iZ_{\rho^*}}(\sqrt{8x}/\sigma)\right],$$

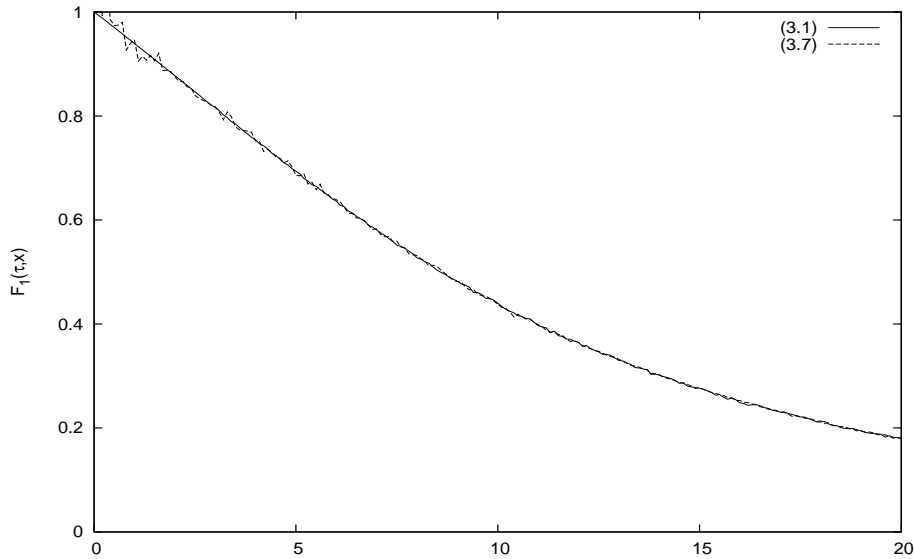$x > 0$, $\tau > 0$, $\rho^* > \rho > 0$. $\square$

Figure 3.3: Computation of $F_1(\tau, x)$ by (3.1) and (3.7) with $x = 0.06$, $\sigma = 0.3$, and $\rho^* = 50$.

A comparison of the graphs obtained by (3.1) and (3.7) is presented in Figure 3.3 with $\rho^* = 50$, a root mean square error of 0.960392 for (3.7) and a root mean square error of 8.81E-3 for (3.1), representing an improvement by a factor 110, for a similar computation time.

A significant variance reduction can be observed in (3.7) when ρ^* becomes larger, although ρ^* cannot be taken too large as the variance

$$E[Z_{\rho^*}^2] = -\frac{\partial^2}{\partial u^2}(\cosh u)_{u=0}^{-\rho^*} = \rho^*$$

of Z_{ρ^*} grows linearly with ρ^*.

(*ii*) <u>Control variate method</u>

Using the relation

$$1 = \Gamma(\rho)\left(\frac{\sigma}{\sqrt{8x}}\right)^\rho E\left[Z_\rho^2 \mathrm{sinhc}(Z_\rho)K_{iZ_\rho}(\sqrt{8x}/\sigma)\right], \qquad x > 0,$$

that follows from (3.2) for $\tau = 0$, we obtain the following proposition.

Proposition 3.2 *For all functions $f : \mathbb{R}_+ \times \mathbb{R} \to \mathbb{R}$ we have*

$$F_\rho(\tau, x) = f(\tau, x)e^{-\sigma^2\tau\rho^2/8}$$
$$+\Gamma(\rho)\left(\frac{\sigma}{\sqrt{8x}}\right)^\rho e^{-\sigma^2\tau\rho^2/8}E\left[Z_\rho^2(e^{-\sigma^2\tau Z_\rho^2/8} - f(\tau, x))\mathrm{sinhc}(Z_\rho)K_{iZ_\rho}(\sqrt{8x}/\sigma)\right].$$

$x > 0, \tau > 0$.

Proof. We have

$$F_\rho(\tau, x) = \Gamma(\rho)\left(\frac{\sigma}{\sqrt{8x}}\right)^\rho e^{-\sigma^2\tau\rho^2/8}E\left[Z_\rho^2 e^{-\sigma^2\tau Z_\rho^2/8}\mathrm{sinhc}(Z_\rho)K_{iZ_\rho}(\sqrt{8x}/\sigma)\right]$$
$$= f(\tau, x)\Gamma(\rho)\left(\frac{\sigma}{\sqrt{8x}}\right)^\rho e^{-\sigma^2\tau\rho^2/8}E\left[Z_\rho^2\mathrm{sinhc}(Z_\rho)K_{iZ_\rho}(\sqrt{8x}/\sigma)\right]$$
$$+\Gamma(\rho)\left(\frac{\sigma}{\sqrt{8x}}\right)^\rho e^{-\sigma^2\tau\rho^2/8}E\left[Z_\rho^2(e^{-\sigma^2\tau Z_\rho^2/8} - f(\tau, x))\mathrm{sinhc}(Z_\rho)K_{iZ_\rho}(\sqrt{8x}/\sigma)\right]$$
$$= f(\tau, x)e^{-\sigma^2\tau\rho^2/8}$$
$$+\Gamma(\rho)\left(\frac{\sigma}{\sqrt{8x}}\right)^\rho e^{-\sigma^2\tau\rho^2/8}E\left[Z_\rho^2(e^{-\sigma^2\tau Z_\rho^2/8} - f(\tau, x))\mathrm{sinhc}(Z_\rho)K_{iZ_\rho}(\sqrt{8x}/\sigma)\right],$$

$x > 0, \tau > 0$.   □

The optimal value of $f(\tau, x) \in \mathbb{R}$ can be computed by a standard covariance argument, cf. e.g. § 4.5.3 of [1], as

$$f_*(\tau, x) = \frac{\mathrm{Cov}\left(Z_\rho^2 e^{-\sigma^2\tau Z_\rho^2/8}\mathrm{sinhc}(Z_\rho)K_{iZ_\rho}(\sqrt{8x}/\sigma), Z_\rho^2\mathrm{sinhc}(Z_\rho)K_{iZ_\rho}(\sqrt{8x}/\sigma)\right)}{\mathrm{Var}\left[Z_\rho^2\mathrm{sinhc}(Z_\rho)K_{iZ_\rho}(\sqrt{8x}/\sigma)\right]}$$

$$= \frac{E\left[Z_\rho^4 e^{-\sigma^2\tau Z_\rho^2/8}\mathrm{sinhc}^2(Z_\rho)K_{iZ_\rho}^2(\sqrt{8x}/\sigma)\right] - \frac{2^{3\rho/2}}{x^{-\rho/2}}\frac{\pi}{\sigma^\rho\Gamma(\rho)}E\left[Z_\rho^2 e^{-\sigma^2\tau Z_\rho^2/8}\mathrm{sinhc}(Z_\rho)K_{iZ_\rho}(\sqrt{8x}/\sigma)\right]}{E\left[Z_\rho^4\mathrm{sinhc}^2(Z_\rho)K_{iZ_\rho}^2(\sqrt{8x}/\sigma)\right] - 2^{3\rho}x^\rho\pi^2\sigma^{-2\rho}/(\Gamma(\rho))^2}.$$

$$(3.8)$$

It can also be approximated by minimizing

$$E[(e^{-\sigma^2\tau Z_\rho^2/8} - f(\tau, x))^2]$$

i.e.

$$f_*(\tau, x) = E[e^{-\sigma^2\tau Z_\rho^2/8}] = \frac{2^{\rho-1}}{\pi\Gamma(\rho)}\int_0^\infty e^{-\sigma^2\tau x^2/8}\left|\Gamma\left(\frac{\rho}{2} + i\frac{x}{2}\right)\right|^2 dx, \qquad (3.9)$$

which can be approximated by

$$f_*(\tau, x) = e^{-\sigma^2\tau E[Z_\rho^2]/8} \simeq e^{-\sigma^2\tau\rho/8}.$$

However the control variate method is difficult to implement alone due to the difficulty in computing the optimal parameter $f_*(\tau, x)$ by (3.8).

(iii) Importance sampling and control variate

Here we implement the control variate method along with importance sampling, by reusing stored samples for the computation of $f_*(\tau, x)$ in (3.8). For all $\rho^* > \rho > 0$ we have

$$F_\rho(\tau, x) = e^{-\sigma^2\rho^2\tau/8}f(\tau, x)$$
$$+ \frac{2^{-\rho^*}\Gamma(\rho^*)}{\Gamma((\rho^*-\rho)/2)^2}\left(\frac{\sigma}{\sqrt{2x}}\right)^\rho \qquad (3.10)$$
$$\times e^{-\sigma^2\rho^2\tau/8}E\left[Z_{\rho^*}^2(e^{-\sigma^2 Z_{\rho^*}^2\tau/8} - f(\tau, x))\left|B\left(\frac{\rho}{2} + i\frac{Z_{\rho^*}}{2}, \frac{\rho^*-\rho}{2}\right)\right|^2\mathrm{sinhc}(Z_{\rho^*})K_{iZ_{\rho^*}}(\sqrt{8x}/\sigma)\right],$$

where $f(\tau, x)$ is a parameter with optimal value

$$f_*(\tau, x) = \frac{E\left[Z_{\rho^*}^4 e^{-\sigma^2 Z_{\rho^*}^2\tau/8}\left|B\left(\frac{\rho}{2} + i\frac{Z_{\rho^*}}{2}, \frac{\rho^*-\rho}{2}\right)\right|^4\mathrm{sinhc}^2(Z_{\rho^*})K_{iZ_{\rho^*}}^2(\sqrt{8x}/\sigma)\right]}{E\left[Z_{\rho^*}^4\left|B\left(\frac{\rho}{2} + i\frac{Z_{\rho^*}}{2}, \frac{\rho^*-\rho}{2}\right)\right|^4\mathrm{sinhc}^2(Z_{\rho^*})K_{iZ_{\rho^*}}^2(\sqrt{8x}/\sigma)\right] - \frac{\Gamma((\rho^*-\rho)/2)^4}{2^{-2\rho^*}\Gamma(\rho^*)^2}\left(\frac{\sqrt{2x}}{\sigma}\right)^{2\rho}}$$

$$-\frac{\frac{\Gamma((\rho^*-\rho)/2)^2}{2^{-\rho^*}\Gamma(\rho^*)}\left(\frac{\sqrt{2x}}{\sigma}\right)^{\rho}E\left[Z_{\rho^*}^2e^{-\sigma^2Z_{\rho^*}^2\tau/8}\left|\mathrm{B}\left(\frac{\rho}{2}+i\frac{Z_{\rho^*}}{2},\frac{\rho^*-\rho}{2}\right)\right|^2\mathrm{sinhc}(Z_{\rho^*})K_{iZ_{\rho^*}}(\sqrt{8x}/\sigma)\right]}{E\left[Z_{\rho^*}^4\left|\mathrm{B}\left(\frac{\rho}{2}+i\frac{Z_{\rho^*}}{2},\frac{\rho^*-\rho}{2}\right)\right|^4\mathrm{sinhc}^2(Z_{\rho^*})K_{iZ_{\rho^*}}^2(\sqrt{8x}/\sigma)\right]-\frac{\Gamma((\rho^*-\rho)/2)^4}{2^{-2\rho^*}\Gamma(\rho^*)^2}\left(\frac{\sqrt{2x}}{\sigma}\right)^{2\rho}}$$

Finally in the next Figure 3.4 we present an implementation of (1.7) using importance sampling and the control variate method, while reusing stored samples of Z_{ρ^*}. We note that the level of precision obtained is comparable to that of the Monte Carlo method (3.1), cf. Figure 3.2, for a similar computation time.
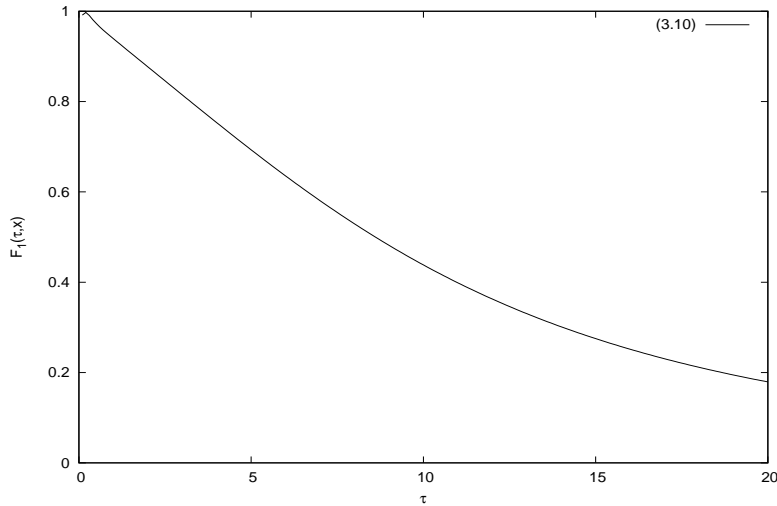

Figure 3.4: Comparison of (3.1) and (3.10) with $x = 0.06$, $\rho = 1$, $\sigma = 0.3$, and $\rho^* = 50$.

Conclusion

In this study, numerical simulations have been performed for the Laplace transform $F_\rho(\tau, x)$ of exponential Brownian functionals using both integral representations and the Monte Carlo method. In the integral method, difficulties in computing (2.2) arose from the function $\theta(\tau, x)$ for which we have confirmed the findings of [7]. Equation (2.5), however, proved less difficult to compute numerically due using existing codes for the evaluation of special functions.

Concerning the computation of $F_\rho(\tau, x)$ by the Monte Carlo method when $\rho > 0$, it has been noticed that for large values of τ, more fluctuations in the values of $F_\rho(\tau, x)$ are present in the standard expression (3.1) than in the hyperbolic secant estimator (3.2), as evidenced by the respective root mean square errors. However, the opposite

holds true for small values of τ as the variance of the hyperbolic secant weight Z_ρ tends to degrade the performance of (3.2) in that case. Variance reduction schemes such as importance sampling and control variate method, along with the reuse of stored samples of Z_ρ, have been found to significantly improve the Monte Carlo estimate.

Acknowledgement

References

[1] P. Brandimarte. *Numerical methods in finance and economics*. Statistics in Practice. Wiley-Interscience [John Wiley & Sons], Hoboken, NJ, second edition, 2006.

[2] P. Carr and M. Schröder. Bessel processes, the integral of geometric Brownian motion, and Asian options. *Theory Probab. Appl.*, 48(3):400–425, 2004.

[3] A. Comtet, C. Monthus, and M. Yor. Exponential functionals of Brownian motion and disordered systems. *J. Appl. Probab.*, 35(2):255–271, 1998.

[4] L. Devroye. A simple algorithm for generating random variates with a log-concave density. *Computing*, 33(3-4):247–257, 1984.

[5] L. Devroye. On random variate generation for the generalized hyperbolic secant distributions. *Statistics and Computing*, 3(3):125–134, 1993.

[6] D. Dufresne. The integral of geometric Brownian motion. *Adv. in Appl. Probab.*, 33(1):223–241, 2001.

[7] K. Ishiyama. Methods for evaluating density functions of exponential functionals represented as integrals of geometric Brownian motion. *Methodol. Comput. Appl. Probab.*, 7(3):271–283, 2005.

[8] P. L'Ecuyer. Uniform random number generators. In M. Lovric, editor, *International Encyclopedia of Statistical Science*. Springer-Verlag, 2010.

[9] F. Lee. Analytical solutions and approximations for the valuation of zero-coupon bonds. Master Thesis, City University of Hong Kong, 2010.

[10] V. Linetsky. Spectral expansions for Asian (average price) options. *Oper. Res.*, 52(6):856–867, 2004.

[11] H. Matsumoto and M. Yor. Exponential functionals of Brownian motion. I. Probability laws at fixed time. *Probab. Surv.*, 2:312–347 (electronic), 2005.

[12] C. Pintoux and N. Privault. A direct solution to the Fokker-Planck equation for exponential Brownian functionals. *Analysis and Applications*, 8(3):287–304, 2010.

[13] C. Pintoux and N. Privault. The Dothan pricing model revisited. *Math. Finance*, 21:355–363, 2011.

[14] A. Schenzle and H. Brand. Multiplicative stochastic processes in statistical physics. *Phys. Rev. A*, 20(4):1628–1647, 1979.

[15] G. N. Watson. *A treatise on the theory of Bessel functions.* Cambridge University Press, Cambridge, 1995. Reprint of the second (1944) edition.

[16] M. Yor. On some exponential functionals of Brownian motion. *Adv. in Appl. Probab.*, 24(3):509–531, 1992.

[17] S. Zhang and J. Jin. *Computation of special functions.* John Wiley & Sons Inc., New York, 1996.